Modeling of advanced electrolyzers: a system simulation approach. Int. J. Hydrogen Energy

Article *in* International Journal of Hydrogen Energy · January 2003

DOI: 10.1016/S0360-3199(02)00033-2

1 author:

Øystein Ulleberg
Institute for Energy Technology
36 PUBLICATIONS **612** CITATIONS

PERGAMON

International Journal of Hydrogen Energy 28 (2003) 21–33

International Journal of HYDROGEN ENERGY

www.elsevier.com/locate/ijhydene

Modeling of advanced alkaline electrolyzers: a system simulation approach

Øystein Ulleberg [1]

Institute for Energy Technology, P.O. Box 40, N-2027 Kjeller, Norway

Abstract

A mathematical model for an advanced alkaline electrolyzer has been developed. The model is based on a combination of fundamental thermodynamics, heat transfer theory, and empirical electrochemical relationships. A dynamic thermal model has also been developed. Comparisons between predicted and measured data show that the model can be used to predict the cell voltage, hydrogen production, efficiencies, and operating temperature. The reference system used was the stand-alone photovoltaic-hydrogen energy plant in Jülich. The number of required parameters has been reduced to a minimum to make the model suitable for use in integrated hydrogen energy system simulations. The model has been made compatible to a transient system simulation program, which makes it possible to integrate hydrogen energy component models with a standard library of thermal and electrical renewable energy components. Hence, the model can be particularly useful for (1) system design (or redesign) and (2) optimization of control strategies. To illustrate the applicability of the model, a 1-year simulation of a photovoltaic-hydrogen system was performed. The results show that improved electrolyzer operating strategies can be identified with the developed system simulation model.

Keywords: Alkaline electrolyzer; Hydrogen systems; Stand-alone power; Renewable energy; Modeling; System simulation

1. Introduction

1.1. Background

Hydrogen is often referred to as the *energy carrier of the future* because it can be used to store intermittent renewable energy (RE) sources such as solar and wind energy. The idea of creating *sustainable energy systems* lead over the past decade to several hydrogen energy demonstration projects around the world [1]. The main objectives of these hydrogen projects was to test and develop components, demonstrate technology, and perform system studies on two categories of systems: (1) stand-alone power systems and (2) hydrogen refueling stations. In the latter category, the most notable project is the hydrogen refueling station at Munich Airport [2]. Most of the previous RE/H_2-projects have been based on solar energy from photovoltaics (PV). However, lately also wind energy conversion systems (WECS) have been considered to be a possible power source, particularly for weak-grid applications.

In all of the cases mentioned above the electrolyzer is a crucial component, and the technical challenge is to make it operate smoothly with intermittent power from renewable energy sources. Up until now most of the R&D on water electrolysis related to RE/H_2-projects have focused on alkaline systems, although there have been some major research efforts on proton exchange membrane (PEM) electrolyzers as well, particularly within the Japanese WE-NET program [3]. However, the costs associated with PEM-electrolysis are still too high, and the market for small-scale H_2-production units is at present day still relatively small.

Institute for Energy Technology (IFE) has since the early 1990s been carrying out theoretical and practical research

[1] Temporary address until 31.12.2002: Murdoch University, South Street, WA, Perth 6150, Australia.

E-mail address: oysteinu@ife.no (Ø. Ulleberg).

0360-3199/02/$ 22.00
PII: S0360-3199(02)00033-2

Nomenclature

Acronyms

AC	alternating current
DC	direct current
EES	Engineering Equation Solver
FZJ	ForschungsZentrum Jülich
HYSOLAR	HYdrogen SOLAR
IEA	International Energy Agency
IFE	Institute for Energy Technology
JANAF	Joint Army-Navy-Air Force (database for thermochemical properties)
KOH	potassium hydroxide
MPPT	maximum power point tracker
PEM	proton exchange membrane
PHOEBUS	PHOtovoltaik-Elektrolyse-Brennstoffzelle Und Systemtecknik
PV	photovoltaic
R&D	research and development
RE	renewable energy
RMS	root mean square
SAPS	stand-alone power system
SIMELINT	SIMulation of Electrolyzers in INTermittent operation
TRNSYS	TRaNsient SYstem Simulation program
WECS	wind energy conversion system
WE-NET	World Energy-Network

Symbols

A	area of electrode, m^2
aq	water based solution
C_{cw}	thermal capacity of cooling water, J K^{-1}
C_t	overall thermal capacity of electrolyzer, J K^{-1}
emf	electromotive force, V
f_1	parameter related to Faraday efficiency, mA^2 cm^{-4}
f_2	parameter related to Faraday efficiency
g	gas
h_{cond}	parameter related to conduction heat transfer, W K^{-1}
h_{conv}	parameter related to convection heat transfer, W K^{-1} A^{-1}
I	current, A
l	liquid
LMTD	log mean temperature difference, °C
n_c	number of cells in series per stack
p	pressure, bar
r	parameter related to ohmic resistance of electrolyte, $\Omega\ m^2$
R_t	overall thermal resistance of electrolyzer, W^{-1} K
s	coefficient for overvoltage on electrodes, V
t	coefficient for overvoltage on electrodes, A^{-1} m^2
SOC	state of charge (battery), 0 … 1
T	temperature, K or °C
U	voltage, V
UA_{HX}	overall heat transfer coefficient-area product for heat exchanger, W^{-1} K
ΔG	change in Gibbs energy, J mol^{-1}
ΔH	change in enthalpy, J mol^{-1}
ΔS	change in entropy, J K^{-1} mol^{-1}
$\dot{n}$	molar flow rate, mol/s
$\dot{Q}$	heat transfer rate, W
Δt	time interval, s

Subscripts

a	ambient
cool	cooling (auxiliary)
cw	cooling water
gen	generated
H_2	pure hydrogen
H_2O	pure water
i, o	inlet, outlet
ini	initial
loss	loss to ambient
O_2	pure oxygen
rev	reversible

Constants

F	96 485 C mol^{-1} or As mol^{-1} Faraday constant
z	2 number of electrons transferred per reaction
R	8.315 J K^{-1} mol^{-1} universal gas constant
v_{std}	0.0224136 m^3 mol^{-1} volume of an ideal gas at standard conditions

in the area of stand-alone power systems (SAPS) based on RE sources and H_2-technology [4–6], and joined in 1999 the IEA Hydrogen Program Annex 13 [7]. The electrolyzer modeling efforts performed in this context focused on alkaline electrolysis, as this was the technology chosen for the relevant applications. It is this modeling effort that is being reported in this paper. However, it should be noted that IFE is currently in the process of acquiring a small-scale PEM-electrolyzer unit for testing in a laboratory setup, which hopefully will give valuable system performance data over the next 2–3 years. The theory and modeling philosophy presented here could be applied to the PEM-technology.

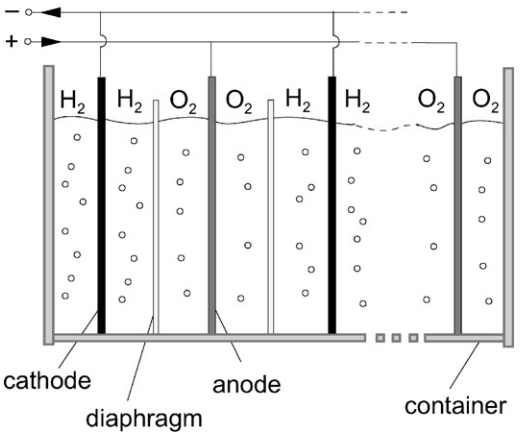

Fig. 1. Principle of a monopolar electrolyzer design.

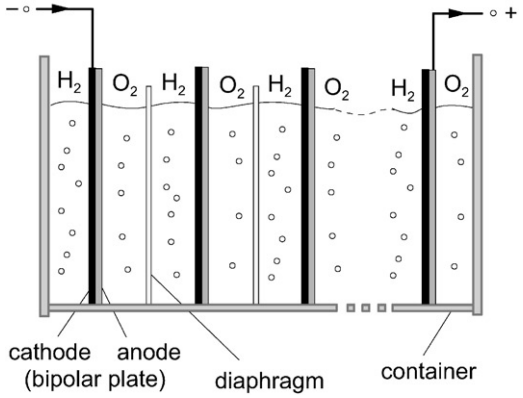

Fig. 2. Principle of a bipolar electrolyzer design.

Over the past decade there has been an increasing interest in system analysis of integrated RE/H_2-systems, especially among those energy and utility companies that are trying to position themselves in the future markets of distributed power generation and alternative fuels. Therefore, there is a need for an electrolyzer model that is suitable for dynamic simulation of such systems. There is also a need for a model with a relatively high level of detail. One particularly important requirement is that the technical model can be coupled to economic models that account for both investment and operational costs.

1.2. Technology

The electrolyte used in the conventional alkaline water electrolyzers has traditionally been aqueous potassium hydroxide (KOH), mostly with solutions of 20–30 wt% because of the optimal conductivity and remarkable corrosion resistance of stainless steel in this concentration range [8]. The typical operating temperatures and pressures of these electrolyzers are 70–100°C and 1–30 bar, respectively.

Physically an electrolyzer stack consists of several cells linked in series. Two distinct cell designs does exist: *monopolar* and *bipolar* [9]. In the monopolar design the electrodes are either negative or positive with parallel electrical connection of the individual cells (Fig. 1), while in the bipolar design the individual cells are linked in series electrically and geometrically (Fig. 2). One advantage of the bipolar electrolyzer stacks is that they are more compact than monopolar systems. The advantage of the compactness of the bipolar cell design is that it gives shorter current paths in the electrical wires and electrodes. This reduces the losses due to internal ohmic resistance of the electrolyte, and therefore increases the electrolyzer efficiency. However, there are also some disadvantages with bipolar cells. One example is the parasitic currents that can cause corrosion problems. Furthermore, the compactness and high pressures of the bipolar electrolyzers require relatively sophisticated and complex system designs, and consequently increases the manufacturing costs. The relatively simple and sturdy monopolar electrolyzers systems are in comparison less costly to manufacture. Nevertheless, most commercial alkaline electrolyzers manufactured today are bipolar.

In new *advanced alkaline electrolyzers* the operational cell voltage has been reduced and the current density increased compared to the more conventional electrolyzers. Reducing the cell voltage reduces the unit cost of electrical power and thereby the operation costs, while increasing the current density reduces the investment costs [8]. However, there is a conflict of interest here because the ohmic resistance in the electrolyte increases with increasing current due to increasing gas bubbling. Increased current densities also lead to increased overpotentials at the anodes and cathodes.

Three basic improvements can be implemented in the design of advanced alkaline electrolyzers: (1) new cell configurations to reduce the surface-specific cell resistance despite increased current densities (e.g., *zero-gap cells* and low-resistance diaphragms), (2) higher process temperatures (up to 160°C) to reduce the electric cell resistance in order to increase the electric conductivity of the electrolyte, and (3) new electrocatalysts to reduce anodic and cathodic overpotentials (e.g., mixed-metal coating containing cobalt oxide at anode and Raney-nickel coatings at cathode). In the *zero-gap cell* design the electrode materials are pressed on either side of the diaphragm so that the hydrogen and oxygen gases are forced to leave the electrodes at the rear. Most manufacturers have adopted this design [9].

1.3. Modeling

Most of the relevant electrolyzer modeling found in the literature is related to solar-hydrogen demonstration projects from the past decade. The most detailed model to date is probably the SIMELINT-program, developed as part of the Saudi Arabian–German HYSOLAR-project [10]. This

program, which was validated against measured data, accurately predicts the thermal behavior, cell voltage, gas purities, and efficiencies for any given power or current profile. Other empirical models have also been developed [11–15], but these have either been less detailed or not tested and verified against experimental data.

The objective of the work described in this paper has been to develop a model that accurately predicts the electrochemical and thermal dynamic behavior of an advanced alkaline electrolyzer. The model is primarily intended for use in integrated renewable energy systems simulations studies that comprise subsystems such as PV-arrays, WECS, electrolyzers, fuel cells, and hydrogen storage. A few key requirements were placed upon the model; it needed to be numerically robust, versatile and practical to use. Hence, the model needed to be a trade-off between simple and complex modeling. For instance, empirical relations are used to model the most complex electrochemical processes. At the same time, a significant effort has been made to minimize the number of required parameters required by the empirical relations. In order to make the model as generic as possible, fundamental thermodynamics and heat transfer theory is used where appropriate.

The electrolyzer model presented is written as a FORTRAN subroutine primarily designed to run with the simulation programs TRNSYS and EES, but the model has also been designed so that it readily can be integrated into other simulation programs (e.g., MATLAB® Simulink®). TRNSYS is a transient systems simulation program with a modular structure [16]. The TRNSYS library includes many of the components commonly found in thermal and electrical renewable energy systems, as well as component routines to handle input of weather data or other time-dependent forcing functions. The modular structure of TRNSYS gives the program the desired flexibility, as it facilitates for the addition of mathematical models not included in the standard library. The program is well suited to perform detailed analyses of systems whose behavior is dependent on the passage of time. EES, an engineering equation solver, has built-in functions for thermodynamic and transport properties of many substances, including steam, air, refrigerants, cryogenic fluids, JANAF table gases, hydrocarbons and psychrometrics [17]. Additional property data can be added, and the program allows user-written functions, procedures, modules, and tabular data. In this study EES was used to perform parameter sensitivity analyses and to test and verify the model against measured data, while TRNSYS was used to perform integrated system simulations.

2. Model description

The decomposition of water into hydrogen and oxygen can be achieved by passing an electric current (DC) between two electrodes separated by an aqueous electrolyte with good ionic conductivity [9]. The total reaction for splitting water is

$$H_2O(l) + \text{electrical energy} \rightarrow H_2(g) + \tfrac{1}{2}O_2(g). \quad (1)$$

For this reaction to occur a minimum electric voltage must be applied to the two electrodes. This minimum voltage, or *reversible voltage*, can be determined from Gibbs energy for water splitting (described below). In an alkaline electrolyzer the electrolyte is usually aqueous potassium hydroxide (KOH), where the potassium ion K^+ and hydroxide ion OH^- take care of the ionic transport. The anodic and cathodic reactions taking place here are

$$\text{Anode}: \quad 2OH^-(aq) \rightarrow \tfrac{1}{2}O_2(g) + H_2O(l) + 2e^-, \quad (2)$$

$$\text{Cathode}: \quad 2H_2O(l) + 2e^- \rightarrow H_2(g) + 2OH^-(aq). \quad (3)$$

In an alkaline solution the electrodes must be resistant to corrosion, and must have good electric conductivity and catalytic properties, as well as good structural integrity, while the diaphragm should have low electrical resistance. This can, for instance, be achieved by using anodes based on nickel, cobalt, and iron (Ni, Co, Fe), cathodes based on nickel with a platinum activated carbon catalyst (Ni, C–Pt), and nickel oxide (NiO) diaphragms. Fig. 3 illustrates the operation principle of alkaline water electrolysis.

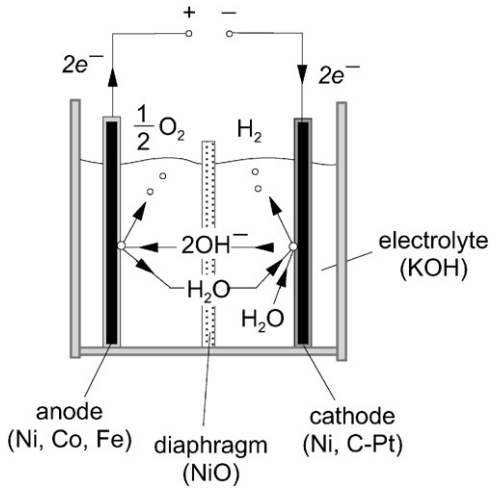

Fig. 3. Operation principle of alkaline water electrolysis.

2.1. Thermodynamic model

Thermodynamics provides a framework for describing reaction equilibrium and thermal effects in electrochemical reactors. It also gives a basis for the definition of the driving forces for transport phenomena in electrolytes and leads to the description of the properties of the electrolyte solutions [18]. Details on the fundamental equations for electrochemical reactors, or electrolyzers, are found in the basic literature [19]. Below is a brief description of the thermodynamics of the low-temperature hydrogen–oxygen electrochemical

reactions used in the electrolyzer model. (A maximum electrolyzer temperature of 100°C was assumed in this study.)

The following assumptions can be made about the water splitting reaction: (a) hydrogen and oxygen are ideal gases, (b) water is an incompressible fluid, and (c) the gas and liquid phases are separate. Based on these assumptions the change in enthalpy ΔH, entropy ΔS, and Gibbs energy ΔG of the water splitting reaction can be calculated with reference to pure hydrogen (H_2), oxygen (O_2), and water (H_2O) at standard temperature and pressure (25°C and 1 bar). The total change in enthalpy for splitting water is the enthalpy difference between the products (H_2 and O_2) and the reactants (H_2O). The same applies for the total change in entropy. The change in Gibbs energy is expressed by

$$\Delta G = \Delta H - T\Delta S. \tag{4}$$

At standard conditions (25° and 1 bar) the splitting of water is a *non-spontaneous* reaction, which means that the change in Gibbs energy is positive. The standard Gibbs energy for water splitting is $\Delta G^\circ = 237\ \text{kJ mol}^{-1}$. For an electrochemical process operating at constant pressure and temperature the maximum possible useful work (i.e., the reversible work) is equal to the change in Gibbs energy ΔG. Faraday's law relates the electrical energy (emf) needed to split water to the chemical conversion rate in molar quantities. The emf for a reversible electrochemical process, or the *reversible cell voltage*, is expressed by

$$U_{\text{rev}} = \frac{\Delta G}{zF}. \tag{5}$$

The total amount of energy needed in water electrolysis is equivalent to the change in enthalpy ΔH. From Eq. (4) it is seen that ΔG includes the thermal irreversibility $T\Delta S$, which for a reversible process is equal to the heat demand. The standard enthalpy for splitting water is $\Delta H^\circ = 286\ \text{kJ mol}^{-1}$. The total energy demand ΔH is related to the *thermoneutral cell voltage* by the expression

$$U_{\text{tn}} = \frac{\Delta H}{zF}. \tag{6}$$

At standard conditions $U_{\text{rev}} = 1.229$ V and $U_{\text{tn}} = 1.482$, but these will change with temperature and pressure. In the applicable temperature range U_{rev} decreases slightly with increasing temperature ($U_{\text{rev@80°C, 1 bar}} = 1.184$ V), while U_{tn} remains almost constant ($U_{\text{tn@80°C, 1 bar}} = 1.473$ V). Increasing pressure increases U_{rev} slightly ($U_{\text{rev@25°C, 30 bar}} = 1.295$ V), while U_{tn} remains constant.

2.2. Electrochemical model

The electrode kinetics of an electrolyzer cell can be modeled using empirical current–voltage (I–U) relationships. Several empirical I–U models for electrolyzers have been suggested [11,13,14,20]. The basic form of the I–U curve used in this study is, for a given temperature

$$U = U_{\text{rev}} + \frac{r}{A}I + s\log\left(\frac{t}{A}I + 1\right). \tag{7}$$

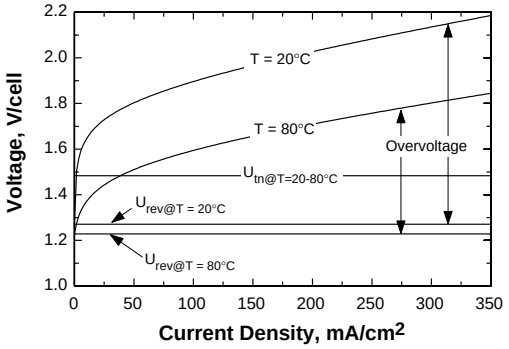

Fig. 4. Typical I–U curves for an electrolyzer cell at high and low temperatures.

Fig. 4 shows the cell voltage versus the current density at a high and low operation temperature for a typical alkaline water electrolyzer. As seen, the difference between the two I–U curves is mainly due to the temperature dependence of the overvoltages.

In order to properly model the temperature dependence of the overvoltages (Eq. (7)) can be modified into a more detailed I–U model, which takes into account the temperature dependence of the ohmic resistance parameter r and the overvoltage coefficients s and t. A temperature dependent I–U model has been proposed by the author [21]:

$$U = U_{\text{rev}} + \frac{r_1 + r_2 T}{A}I + s\log\left(\frac{t_1 + t_2/T + t_3/T^2}{A}I + 1\right). \tag{8}$$

The Faraday efficiency is defined as the ratio between the actual and theoretical maximum amount of hydrogen produced in the electrolyzer. Since the Faraday efficiency is caused by parasitic current losses along the gas ducts, it is often called the *current efficiency*. The parasitic currents increase with decreasing current densities due to an increasing share of electrolyte and therefore also a lower electrical resistance [20]. Furthermore, the parasitic current in a cell is linear to the cell potential (Eq. (8)). Hence, the fraction of parasitic currents to total current increases with decreasing current densities. An increase in temperature leads to a lower resistance, more parasitic currents losses, and lower Faraday efficiencies. An empirical expression that accurately depicts these phenomena for a given temperature is

$$\eta_{\text{F}} = \frac{(I/A)^2}{f_1 + (I/A)^2} f_2. \tag{9}$$

According to Faraday's law, the production rate of hydrogen in an electrolyzer cell is directly proportional to the

transfer rate of electrons at the electrodes, which in turn is equivalent to the electrical current in the external circuit. Hence, the total hydrogen production rate in an electrolyzer, which consists of several cells connected in series, can be expressed as

$$\dot{n}_{H_2} = \eta_F \frac{n_c I}{zF}. \tag{10}$$

The water consumption and oxygen production rates are simply found from stoichiometry (Eq. (1)), which on a molar basis [2] is

$$\dot{n}_{H_2O} = \dot{n}_{H_2} = 2\dot{n}_{O_2}. \tag{11}$$

The generation of heat in an electrolyzer is mainly due to electrical inefficiencies. The *energy efficiency* can be calculated from the thermoneutral voltage (Eq. (6)) and the cell voltage (Eq. (8)) by the expression

$$\eta_e = \frac{U_{tn}}{U}. \tag{12}$$

For a given temperature, an increase in hydrogen production (i.e., an increase in current density) increases the cell voltage (Fig. 4), which consequently decreases the energy efficiency. For a given current density, the energy efficiency increases with increasing cell temperature. It should be noted here that Eq. (12) is only valid for systems where no auxiliary heat is added to the system. (If auxiliary heat is added, the voltage may, at very low current densities, drop into the region between the reversible and thermoneutral voltage, and the efficiency would be greater than 100%). In low-temperature electrolysis, the cell voltage will during normal operation (50–80 °C and 40–300 mA cm^{-2}) always be well above the thermoneutral voltage, as observed in Fig. 4. However, some initial heating may be required during start-up if the electrolyzer has been allowed to cool down to ambient temperature ($\sim$ 20 °C).

In order to calculate the overall performance of an electrolyzer system, information about the number of cells in series and/or parallel per stack and the number of stacks per unit is needed. The rated voltage of an electrolyzer stack is found from the number of cells in series, while the number of cells in parallel yields the rated current (and H_2-production). The total power is simply the product of the current and voltage.

2.3. Thermal model

The temperature of the electrolyte of the electrolyzer can be determined using simple or complex thermal models, depending on the need for accuracy. Assuming a lumped thermal capacitance model [22], the overall thermal energy balance can be expressed as

$$C_t \frac{dT}{dt} = \dot{Q}_{gen} - \dot{Q}_{loss} - \dot{Q}_{cool}, \tag{13}$$

where

$$\dot{Q}_{gen} = \eta_c (U - U_{tn}) I = n_c U I (1 - \eta_e), \tag{14}$$

$$\dot{Q}_{loss} = \frac{1}{R_t}(T - T_a), \tag{15}$$

$$\dot{Q}_{cool} = C_{cw}(T_{cw,i} - T_{cw,o}) = UA_{HX}\,LMTD \tag{16}$$

and

$$LMTD = \frac{(T - T_{cw,i}) - (T - T_{cw,o})}{\ln[(T - T_{cw,i})/(T - T_{cw,o})]}. \tag{17}$$

The first term on the right-hand side of Eq. (13) is the internal heat generation, the second term the total heat loss to the ambient, and the third term the auxiliary cooling demand. The overall thermal capacity C_t and resistance R_t for the electrolyzer, and the UA-product for the cooling water heat exchanger are the constants that need to be determined analytically or empirically prior to solving the thermal equations. It should be noted that the thermal model presented here is on a per stack basis.

A simple method to calculate the electrolyzer temperature is to assume constant heat generation and heat transfer rates for a given time interval. If the time steps are chosen sufficiently small, the result is a quasi steady-state thermal model. Using Eq. (13) as the basis, a quasi steady-state thermal model can be expressed as

$$T = T_{ini} + \frac{\Delta t}{C_t}(\dot{Q}_{gen} - \dot{Q}_{loss} - \dot{Q}_{cool}). \tag{18}$$

A more complex method is to solve the differential equation analytically and calculate the temperature directly. However, for this to be possible an expression for the outlet cooling water must first be found. If a constant temperature in the LMTD-expression above is assumed, Eq. (16) can be rewritten to

$$T_{cw,o} = T_{cw,i} + (T - T_{cw,i})\left[1 - \exp\left(-\frac{UA_{HX}}{C_{cw}}\right)\right]. \tag{19}$$

Using Eq. (13) as the basis and inserting Eqs. (14)–(16) and (19), it can be demonstrated that the overall thermal energy balance on the electrolyzer can be expressed by the linear, first-order, non-homogeneous differential equation

$$\frac{dT}{dt} + aT - b = 0 \tag{20}$$

with solution

$$T(t) = \left(T_{ini} - \frac{b}{a}\right)\exp(-at) + \frac{b}{a}, \tag{21}$$

[2] Gas flow rates are commonly given on a normal cubic meter per hour (Nm^3 h^{-1}) basis (Eq. (A.1)).

where

$$a = \frac{1}{\tau_t} + \frac{C_{cw}}{C_t}\left[1 - \exp\left(-\frac{UA_{HX}}{C_{cw}}\right)\right], \quad (22)$$

$$b = \frac{n_c UI(1-\eta_e)}{C_t} + \frac{T_a}{\tau_t} + \frac{C_{cw}T_{cw,i}}{C_t}\left[1 - \exp\left(-\frac{UA_{HX}}{C_{cw}}\right)\right]. \quad (23)$$

One advantage of having an analytical expression for the temperature is that it facilitates the determination of the thermal time constant ($\tau_t = R_t C_t$). It also provides a means to double check a numerical solution of the differential equation.

In an alkaline electrolyzer with a stationary electrolyte, it has been observed that the overall UA-product for the cooling water heat exchanger is (indirectly) a function of the electrical current required by the electrolyzer (Fig. 10). Hence, an empirical expression that accounts for both conduction and convection heat transfer phenomena is proposed:

$$UA_{HX} = h_{cond} + h_{conv} I. \quad (24)$$

The physical explanation for this behavior is that since the electrolyte is stationary, and no pump is being used, the convection heat transfer increases as a result of more mixing of the electrolyte. An increase in mixing occurs because the volume of the gas bubbles in the electrolyte increases with increasing current density. Similarly, the ohmic resistance in the electrolyte increases with increasing currents due to increasing gas bubbling. Hence, this behavior is accounted for in Eq. (24) and in the ohmic resistance term of Eq. (8).

3. Testing and verification of model

The alkaline electrolyzer analyzed in this study is the one installed at the PHOEBUS plant in Jülich [23]. It is a so-called *advanced alkaline electrolyzer* that operates at a pressure of 7 bar and at temperatures up to about 80°C. The cells are circular, bipolar (Fig. 1), have a zero spacing geometry, and consist of NiO diaphragms and activated electrodes (Fig. 3), which make them highly efficient. The electrolyte is a stationary 30 wt% KOH solution. Each cell has an electrode area of 0.25 m^2 and there are 21 cells connected in series. This gives an operation voltage in the range 30–40 V.

The hydrogen production and water cooling flow rates for the PHOEBUS electrolyzer was not logged and collected on a regular basis, along with the minutely collected operational data. However, an experiment, where this and other pertinent data was sampled for every 5 min, was performed on June 17, 1996 [24]. It is this 1-day experiment that forms the basis for the comparisons between simulated and measured data presented below.

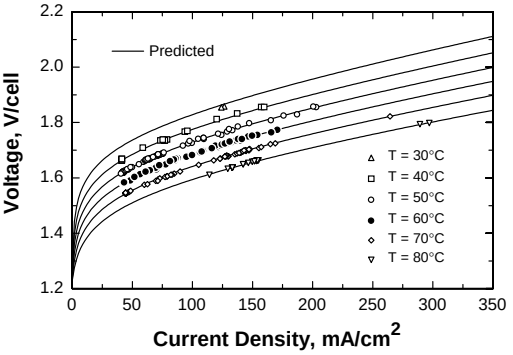

Fig. 5. Predicted versus measured electrolyzer cell voltage.

3.1. Electrochemical model

In order to find the six parameters needed in the proposed empirical *I–U* relationship (Eq. (8)), a systematic strategy for obtaining the best possible curve fit was developed (Appendix A). A comparison between simulated and measured values for current and voltage for various operation temperatures are presented in Fig. 5. The current, voltage, and temperature data base (317 data points) used in Fig. 5 was derived from 3 months (May–July 1996) of operational data for the PHOEBUS electrolyzer.

The results show to which degree the ohmic resistance parameter r is linearly dependent on temperature. Furthermore, the results show that the overvoltage coefficient s can be assumed constant, while the proposed expression for the overvoltage coefficient t can be used. That is, only six parameters are needed to model the *I–U* curve. Fig. 5 demonstrates that the predictability of the proposed *I–U* model in Eq. (8) is excellent; the RMS error is about 2.5 mV $cell^{-1}$.

Detailed measurements of the hydrogen production at various current densities for the PHOEBUS electrolyzer (26 kW, 7 bar) were only available for an operation temperature of 80°C. However, detailed experiments on the temperature sensitivity of the Faraday efficiency were performed on a very similar electrolyzer (10 kW, 5 bar) installed at the HYSOLAR test and research facility for solar hydrogen production in Stuttgart, Germany [20]. A comparison between these two electrolyzers is given in Fig. 6, which shows the data points from the HYSOLAR experiments (performed at temperatures of 40°C, 60°C, and 80°C), the data points for PHOEBUS (80°C), and the corresponding curve fits. Fig. 6 illustrate that the form of the Faraday efficiency expression proposed in Eq. (9) is suitable. A more detailed analysis of the results shows that the coefficients f_1 and f_2 vary linearly with temperature (Appendix A).

In a system simulation study it is important to reduce the number of parameters required. Having this in mind, a simplified Faraday efficiency expression with non-temperature-dependent coefficients (Eq. (9)) was tested. The measured hydrogen production (recorded at

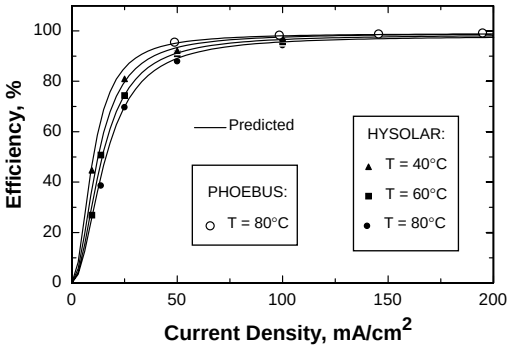

Fig. 6. Predicted versus measured faraday efficiency for two advanced alkaline electrolyzers: (1) PHOEBUS (26 kW, 7 bar) and (2) HYSOLAR (10 kW, 5 bar).

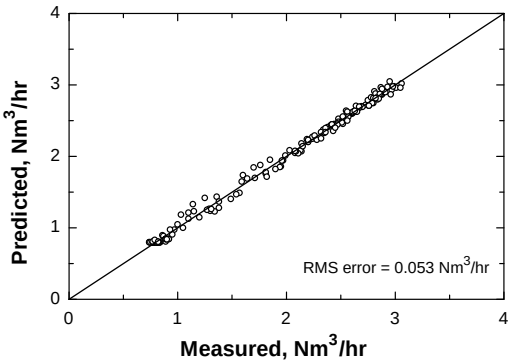

Fig. 7. Predicted versus measured hydrogen production.

5 min intervals over a 15-h time period) was compared to the model. The results (Fig. 7) show that for system simulations it suffices to model the Faraday efficiency with a simple non-temperature-dependent expression. This can be explained by the fact that in an actual system the electrolyzer is always operating above a minimum protective (idling) current (Fig. 9). Hence, the electrolyzer is usually operating in a region where the Faraday efficiency is not significantly affected by a change in temperature. A closer look at the hydrogen production for a typical day with variable electrical current (Figs. 8 and 9) show that there is good agreement between the measured data and the model.

3.2. Thermal model

The cooling of the electrolyzer is crucial to prevent overheating. The most convenient cooling method is usually to use regular tap water, as was the case with the PHOEBUS electrolyzer. The average tap water flow rate and inlet temperature for the specific day discussed here was 0.6 $Nm^3\ h^{-1}$ and 14.5°C, respectively. In order to estimate the cooling effect an overall UA-product for the heat transfer between

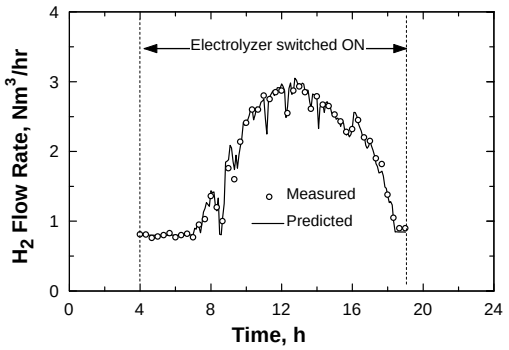

Fig. 8. Predicted versus measured H_2-production for a typical day with variable electrolyzer current input. (For clarity, only every fourth measured data point was plotted).

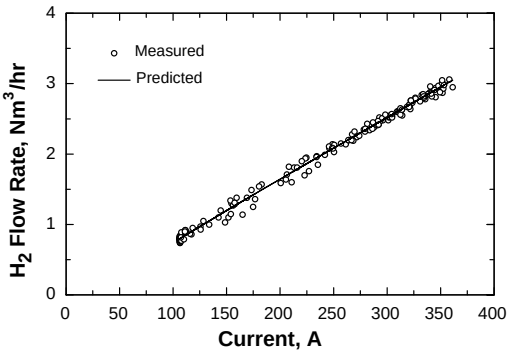

Fig. 9. Predicted and measured H_2-production as a function of measured electrical current. (The same day as shown in Fig. 8, but with all of the data points included).

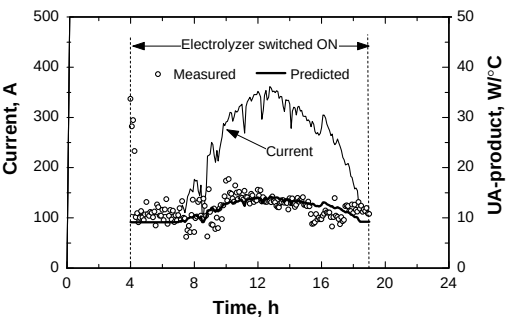

Fig. 10. Overall UA-product for the heat exchanger between the cooling water and the electrolyzer.

the cooling water and the electrolyzer was proposed in Eq. (24). A comparison between the measured and predicted UA-product is given in Fig. 10. The results clearly shows that there exists an indirect relationship between the electrolyzer current and the UA-product, and that this can, to a good approximation, be accounted for by the proposed empirical equation.

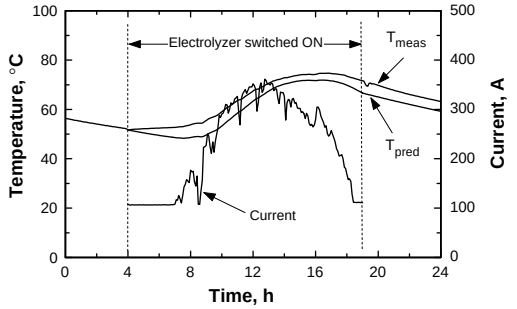

Fig. 11. Predicted versus measured electrolyzer temperature.

The electrolyzer temperature for a day with variable power input (solar energy minus user load) is depicted in Fig. 11. The initial temperature (at midnight) was 56.4°C and the temperature at start-up of the electrolyzer (04:00 AM) was 51.7°C. This initial decrease in temperature is only due to natural cooling to the ambient, with a temperature of about 20°C. The values for the thermal capacitance and for the overall thermal resistance were found by investigating the cooling pattern for electrolyzer for a number of different days: $C_t = 625$ kJ °C^{-1} and $R_t = 0.167$°C W^{-1} (equal to $\tau_t = 29$ h). The heat generation was calculated from the energy efficiency (Eq. (14)), where the electrical current input was based on measurements depicted in Fig. 11, and the auxiliary cooling was based on measured tap water conditions (0.6 Nm^3 h^{-1} and 14.5°C).

The result of this 1-day simulation shows that the model slightly underpredicts the temperature. There might be several explanations for this. One possible reason is measurement error, where the main source of uncertainty is the measured temperature of the electrolyte. Another possible reason is simply the lack of detail in the thermal model, where the main deficiency of the model is that the temperature of the electrolyte is assumed to be homogeneous. However, in general, the thermal dynamic behavior of the electrolyzer is predicted quite accurately.

The importance of modeling the electrolyzer temperature accurately depends on the purpose of the models. A comparison between predicted and measured electrolyzer voltage and the corresponding power shows that the slight underprediction of the temperature has relatively little significance from an energy system simulation point of view. For instance, in the 1-day simulation presented above, the error between the total simulated and measured energy demand was less than 2%.

4. System simulation results

The intention of the electrolyzer model presented in this study is to integrate it with other renewable and hydrogen energy models, and perform system simulation studies. Thus, the usefulness of the model can essentially be divided into two distinct modeling areas: (1) system design (or redesign) and (2) optimization of control strategies.

The applicability of the model is best illustrated by showing some results from integrated system simulations. The reference system (Fig. 12) used in the simulations presented here is the PHOEBUS demonstration plant at the Research Center in Jülich, Germany [23]. At the time of the study this system consisted of four differently oriented PV-arrays with maximum power point trackers (MPPTs), a pressurized advanced alkaline electrolyzer, hydrogen and oxygen storage pressure vessels, an alkaline fuel cell, power conditioning equipment (two DC/DC-converters and one DC/AC-inverter), and a lead acid battery bank.

The level of detail of the electrolyzer model makes it possible to investigate a number of important system performance parameters such as the number of electrolyzer starts, H_2-production, operating time, and standby (idling) time. Statistical data such as minimum, maximum, and average electrolyzer current, voltage, power, flow rates and temperatures can also be analyzed. Comparisons with the reference system show that the model has a suitable level of detail [5].

One of the key system control parameters is the operational mode of the electrolyzer, which determines whether the electrolyzer is to operate in a fixed or variable current mode. In the constant current mode the battery is charged during periods of excess current on the busbar and discharged during periods with deficit current. The battery state of charge (SOC) in this case will mainly depend on two uncontrollable variables, the solar radiation and user load, and one controllable variable, the fixed current (or power) setting of the electrolyzer.

In the variable current scenario only excess current available on the busbar is fed to the electrolyzer, hence the battery SOC remains constant. It is important to note that most alkaline electrolyzers, even advanced ones specifically designed to manage fluctuating input current, can only operate down to about 20% of their rated power, and an idling current needs to be maintained. Table 1 summarizes the result from an analysis made on the influence of alternative electrolyzer control strategies on system performance.

Electrolyzer mode of operation (*fixed or variable*): The benefit of operating the electrolyzer in a variable current mode rather than at a fixed current is illustrated by comparing Sim *A*–Sim *B*. In Sim *B* the electrolyzer was operating at a fixed current of 550 A ($\sim$ 21 kW), which gave a much more frequent electrolyzer on/off-switching than in Sim *A*. This is also reflected in the low average run time. The net result is less hydrogen production, yielding a lower final pressure level in the H_2-storage at the end of the year. In Sim *A*, on the other hand, a large fraction of the energy from the PV-arrays was used directly to run the electrolyzer. As a consequence the use of the battery was minimized. A comparison between Sim *A* and Sim *B* shows that the battery discharging energy increased by about 50%. Other fixed current set points have been investigated [5] and the trend

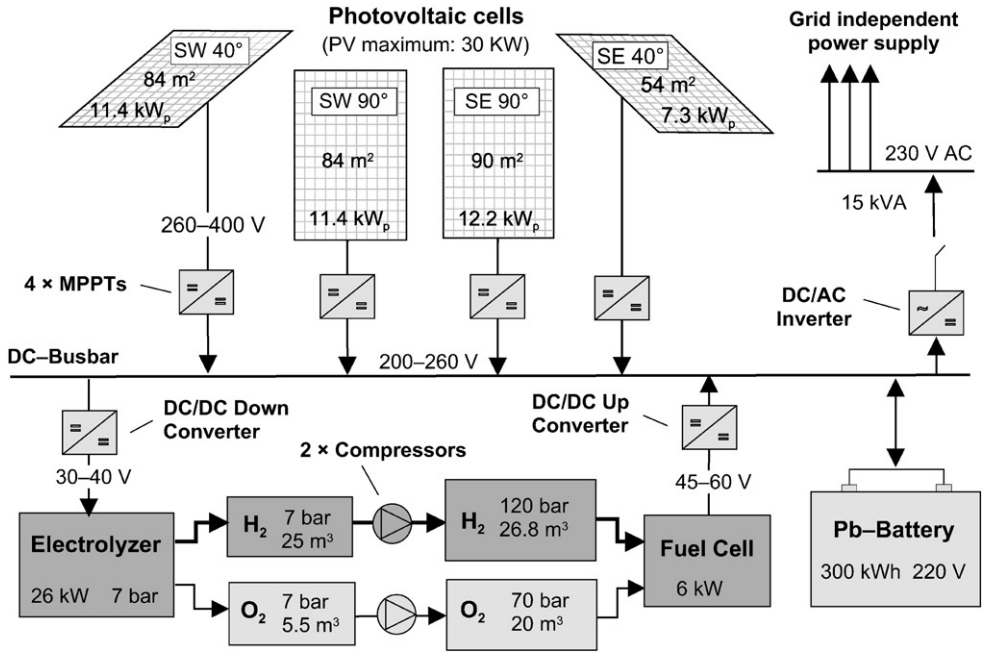

Fig. 12. Reference system (PHOEBUS).

Table 1
Influence of alternative electrolyzer control strategies on system performance

Component/system		Units	Electrolyzer variations		
			A	B	C
Control set points					
Electrolyzer	Fixed current set point (if any)	A	Variable	*550*	Variable
	Battery SOC level for on-switching	%	90	90	*80*
	Battery SOC level for off-switching	%	80	80	*70*
Key performance indicators					
H_2-storage	Initial H_2 storage pressure	0…1	0.45	0.45	0.45
	Final H_2 storage pressure	0…1	0.24	*0.11*	0.20
Performance parameters					
Electrolyzer	Energy consumption	MW h	10.56	9.94	10.83
	Average power	kW	7.48	*21.01*	7.37
	Number of starts	—	156	*273*	162
	Average run time	h	9.0	1.7	9.1
	H_2 production	Nm^3	2,719	2,473	2,788
Battery	Energy, discharging	MW h	9.74	*15.09*	9.54
	Energy, charging	MW h	8.90	*13.68*	8.85

Italics = change in set point or majoreffect due to change in set point.

is the same: variable electrolyzer operation mode gives a better system performance than fixed current mode.

Basic control strategy for electrolyzer: The influence of reducing the upper and lower thresholds for the on/off-switching of the electrolyzer can be seen by comparing Sim *A*–Sim *C*. In Sim *C* the on/off-switching set points were lowered by 10% compared to Sim *A*, which required the battery to operate much more frequently at medium high SOC (60–80%), and less frequently at high SOC levels. Hence, the higher threshold settings used in Sim *A* gave a better utilization of the installed battery capacity. In general, there is a tradeoff between battery capacity utilization on

one hand, and the need to dump energy (at SOC > 100%) on the other. This needs to be incorporated into the control strategy.

5. Conclusions

A mathematical model for an advanced alkaline electrolyzer has been developed based on a combination fundamental thermodynamics, heat transfer theory, and empirical electrochemical relationships. A lumped capacitance thermal dynamic model with a special empirical relationship for the overall heat transfer between a stationary electrolyte and a cooling water loop has also been proposed. Data from a reference system, the stand-alone photovoltaic-hydrogen energy plant (PHOEBUS) in Jülich, was collected. Comparisons between predicted and measured data show that the electrochemical part of the model accurately predicts the cell voltage, hydrogen production, and efficiencies. The results also show that the thermal model can be used to predict the transient behavior of the electrolyzer temperature.

The number of required parameters has been reduced to a minimum so that the model is suitable for use in integrated hydrogen energy system simulations. The electrolyzer model has, along with several other hydrogen energy models such as fuel cells and hydrogen storage, been made compatible to a transient system simulation program (TRNSYS), which makes it possible to integrate hydrogen energy component model with a standard library of thermal and electrical renewable energy components. The model can be particularly useful for (1) system design (or redesign) and (2) optimization of control strategies. To illustrate the applicability of the model, a 1-year simulation of a photovoltaic-hydrogen system was made. The results show that several improved electrolyzer-operating strategies can be identified with the developed system simulation model.

The technical electrolyzer model presented in this paper is suitable for dynamic simulation of RE/H_2-systems. The level of detail in the model is relatively high, but not too high. This means that the model readily can be coupled to economic models that account for both investment and operational costs. Detailed techno-economical system optimization of RE/H_2-systems is the next research topic that will be studied by this author.

Acknowledgements

The work presented in this paper is based a Ph.D.-study carried out at the Institute for Energy Technology (IFE) in conjunction with the Norwegian University of Science and Technology (NTNU). The author would like to thank the Norwegian Research Council (NFR) for the financing (Ph.D. and post.doc.), IFE for providing the necessary research facilities, and the Research Center in Jülich (FZJ) for making the experimental data accessible. A special thanks goes to Jürgen Mergel (FZJ) for being so helpful. A humble thought also goes to my late advisor Professor Odd Andreas Asbjørnsen.

Appendix A.

A.1. Curve fitting

The following systematic seven-step procedure that facilitates the curve fitting of the six parameters needed in the proposed empirical I–U relationship (Eq. (8)) is recommended:

(1) Collect experimental or operational data for current I, voltage U, and temperature T.
(2) Organize the measured values for I and U in sets with respect to constant values for T.
(3) Perform *individual curve fits* of the three coefficients r, s, and t in Eq. (7).
(4) Repeat step (3) for a few other temperatures (e.g., $T = 20^{\circ}$C–80°C).
(5) Perform *intermediate curve fits* on the temperature-dependent coefficients r and t.
(6) Verify that the temperature-dependent coefficients in Eq. (8) behave according to the expressions:

$$r(T) = r_1 + r_2 T \quad \text{and} \quad t_1 + t_2/T + t_3/T^2.$$

(7) Perform an *overall curve fit* on the entire data set, using the values for the parameters r_i, s, and t_i found from steps (1) to (6) as initial values for the regression.

This systematic procedure is illustrated graphically in Fig. 13, which shows the results of individual curve fits at fixed temperatures (data points), intermediate curve fits of these data points (thin lines), and finally the overall curve fit (solid lines). The step-by-step strategy for finding the unknown parameters in Eq. (8) proves to be very robust. This indicates that the approach is not only limited to the curve fitting of the I–U characteristics of an electrolyzer cell, but can also be used in other situations where coefficients in a model are sensitive to inputs such as temperature, pressure, or other governing conditions.

A.2. Parameters

Tables 2–4 list the parameters found and used in this study.

A.3. Equations

Gas flow rates are commonly given on a normal cubic meter per hour ($Nm^3\ h^{-1}$) basis. For ideal gases the conversion from mol s^{-1} to $Nm^3\ h^{-1}$ is given by

$$\dot{V} = \dot{n} v_{\mathrm{std}} 3600, \tag{A.1}$$

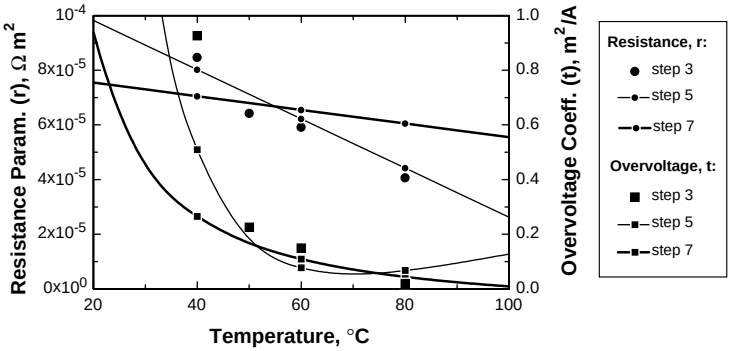

Fig. 13. Electrolyzer I–U curve fitting; illustration of a step-by-step procedure to determine the temperature sensitivity of the resistance parameter r and the overvoltage coefficient t in Eq. (8).

Table 2
I–U curve parameters (Eq. (8))

r_1	$8.05e-5\ \Omega\ m^2$
r_2	$-2.5e-7\ \Omega\ m^2\ ^\circ C^{-1}$
s	0.185 V
t_1	$-1.002\ A^{-1}\ m^2$
t_2	$8.424\ A^{-1}\ m^2\ ^\circ C$
t_3	$247.3\ A^{-1}\ m^2\ ^\circ C^2$

Table 3
Faraday efficiency parameters (Eq. (9))

	PHOEBUS	HYSOLAR			
T	80	40	60	80	°C
f_1	250	150	200	250	$mA^2\ cm^{-4}$
f_2	0.96	0.990	0.985	0.980	0…1

Table 4
UA_{HX} parameters (Eq. (24))

h_{cond}	$7\ W^\circ\ C^{-1}$
h_{conv}	$0.02\ W^\circ\ C^{-1}$ per A

where $\dot{V}$ and $\dot{n}$ are the volumetric and molar flow rates, respectively, and v_{std} is the volume of an ideal gas at standard conditions (0 °C and 1 bar).

The root mean square (RMS) error is calculated according to the equation:

$$\text{RMS error} = \sqrt{\frac{\sum_{i=1}^{n}(\hat{y}_i - y_i)^2}{n-1}}, \qquad (A.2)$$

where $\hat{y}_i$ and y_i are the predicted and measured values, respectively, and n is the number of data points evaluated.

References

[1] Schucan TH. Case studies of integrated hydrogen energy systems. Report, IEA/H2/T11/FR1-2000, International Energy Agency Hydrogen Implementing Agreement Task 11—Integrated Systems. Operating agent: National Renewable Energy Laboratory, Golden, Colorado, 1999.

[2] The Hydrogen project at munich international airport. http://www.hydrogen.org/h2muc/, October 2001.

[3] Yamaguchi M, Shinohara T, Taniguchi H, Nakanori T, Okisawa K. Development of 2500 cm^2 solid polymer electrolyte water electrolyser in WE-NET. Proceedings of the 12th World Hydrogen Energy Congress, Buenos Aires, 21–26 June 1998. p. 747–55.

[4] Galli S, Stefanoni M, Borg P, Brocke WA, Mergel J. Development and testing of a stand-alone small-size solar photovoltaic-hydrogen power system (SAPHYS). Report, JOU2-CT94-0428, JOULE II-Programme, Directorate General XII: Science, Research and Development, European Commission, Brussels, 1997.

[5] Ulleberg Ø. Stand-alone power systems for the future: optimal design, operation and control of solar-hydrogen energy systems. Ph.D. thesis, Norwegian University of Science and Technology, Trondheim, 1998.

[6] Eriksen J, Aaberg RJ, Ulleberg Ø, Ingebretsen F. System analysis of a PEMFC-based stand alone power system (SAPS). First European PEFC Forum, Lucerne, Switzerland, 3–6 July 2001. p. 447–58.

[7] International energy agency (IEA) hydrogen program. Annex 13—design and optimization of integrated systems. http://www.eren.doe.gov/hydrogen/iea/, October 2001.

[8] Wendt H, Plzak H. Hydrogen production by water electrolysis. Kerntechnik 1991;56(1):22–8.

[9] Divisek J. Water electrolysis in low- and medium-temperature regime. In: Wendt H, editor. Electrochemical hydrogen technologies-electrochemical production and combustion of hydrogen. Oxford: Elsevier, 1990.

[10] Hug W, Bussmann H, Brinner A. Intermittent operation and operation modeling of an alkaline electrolyzer. Int J Hydrogen Energy 1993;18(12):973–7.

[11] Griesshaber W, Sick F. Simulation of Hydrogen–Oxygen–Systems with PV for the Self-Sufficient Solar House. FhG-ISE, Freiburg im Breisgau, 1991 (in German).

[12] Ulleberg Ø, Morner SO. TRNSYS simulation models for solar-hydrogen systems. Solar Energy 1997;59(4–6):271–9.
[13] Havre K, Borg P, Tommerberg K. Modeling and control of pressurized electrolyzer for operation in stand alone power systems. Second Nordic Symposium on Hydrogen and Fuel Cells for Energy Storage, Helsinki, January 19–20, 1995. p. 63–78.
[14] Vanhanen J. On the performance improvements of small-scale photovoltaic-hydrogen energy systems. PhD thesis, Helsinki University of Technology, Espoo, Finland, 1996.
[15] Meurer C, Barthels H, Brocke WA, Emonts B, Groehn HG. PHOEBUS—an autonomous supply system with renewable energy: six years of operational experience and advanced concepts. Solar Energy 1999;67(1–3):131–8.
[16] Klein SA, Beckman WA, Mitchell JW, Duffie JA, Duffie NA, Freeman TL, Mitchell JC, Braun JE, Evans BL, Kummer JP, Urban RE, Fiksel A, Thornton JW, Blair NJ, Williams PM, Bradley DE. TRNSYS—a transient system simulation program. Manual v15, Solar Energy Laboratory, University of Wisconsin, Madison, 2000.
[17] Klein SA, Alvarado FL. EES—engineering equation solver. Manual v6.315, F-Chart Software. Middleton: Wisconsin, 2001.
[18] Rousar I. Fundamentals of electrochemical reactors. In: Ismail MI, editor. Electrochemical reactors: their science and technology part A. Amsterdam: Elsevier, 1989.
[19] Pickett DJ. Electrochemical reactor design, 2nd ed. New York: Elsevier, 1979.
[20] Hug W, Divisek J, Mergel J, Seeger W, Steeb H. Highly efficient advanced alkaline electrolyzer for solar operation. Int J Hydrogen Energy 1992;17(9):699–705.
[21] Ulleberg Ø. Simulation of autonomous PV-H2 systems: analysis of the PHOEBUS plant design, operation and energy management. ISES 1997 Solar World Congress, Taejon, August 24–30, 1997.
[22] Incropera FP, DeWitt DP. Fundamentals of heat and mass transfer, 3rd ed. New York: Wiley, 1990.
[23] Barthels H, Brocke WA, Bonhoff K, Groehn HG, Heuts G, Lennartz M, Mai H, Mergel J, Schmid L, Ritzenhoff P. PHOEBUS-Jülich: an autonomous energy supply system comprising photovoltaics, electrolytic hydrogen, fuel cell. Int J Hydrogen Energy 1998;23(4):295–301.
[24] Mergel J. Personal communication, PHOEBUS electrolyzer: detailed operational data. FZJ—Forschungszentrum, Jülich, February 1997.